

Ferromagnetism of GaMnAs studied by polarized neutron reflectometry

H. Kępa,¹ J. Kutner-Pielaszek,¹ A. Twardowski,¹ C. F. Majkrzak,² J. Sadowski,^{3,4} T. Story,³ and T. M. Giebultowicz⁵

¹*Institute of Experimental Physics, Warsaw University, Hoża 69, 00-681 Warszawa, Poland*

²*NIST Center for Neutron Research, Gaithersburg, Maryland 20899*

³*Institute of Physics, Polish Academy of Sciences, Al. Lotników 32/46, 02-668 Warszawa, Poland*

⁴*Department of Experimental Physics, Chalmers University of Technology and Göteborg University, SE-412 96 Göteborg, Sweden*

⁵*Physics Department, Oregon State University, 301 Weniger Hall, Corvallis, Oregon 97331*

(Received 18 June 2001; published 5 September 2001)

Polarized neutron reflectometry has been used to investigate details of spin ordering in ferromagnetic (FM) GaMnAs/GaAs superlattices. The reflectivity spectra measured below the Curie temperature reveal additional magnetic contributions to the structural superlattice Bragg peaks, clearly indicating the existence of FM interlayer correlations. Closer investigation of the magnetic reflectivity maxima using a full polarization analysis provides direct evidence that the FM order in the GaMnAs layers is truly long range. Moreover, as shown by the data, the system exhibits a strong tendency of forming a single-domain FM arrangement, even when cooled through T_C in zero external field.

DOI: 10.1103/PhysRevB.64.121302

PACS number(s): 75.25.+z, 75.50.Pp, 75.75.+a

Currently, a great deal of attention is being focused on a new area of solid-state electronics, usually referred to as “spintronics.”¹ In contrast to conventional electronics, in spintronics not only the current magnitude, but also its spin state is controlled. Spin valves and spin injectors are the first examples of practical application of spintronics. Further progress in developing new devices hinges critically on the availability of suitable materials. Such materials need to be “good” semiconductors, easy to integrate in typical ICs, and their semiconductor properties should exhibit strong sensitivity to the electronic spin states. An especially desirable property is ferromagnetism, as it greatly enhances the effect of an external magnetic field. Unfortunately, there are few natural ferromagnetic semiconductors, and none of them are particularly useful for spintronics applications, due to either too low Curie temperatures (e.g., EuO, EuS) or structural incompatibility with materials typically used in semiconductor technology (e.g., CuCr₂Te₃I). In search of better materials, since the mid-1970s researchers started investigating systems known as diluted magnetic semiconductors (DMS), which are derived from canonical semiconductors (such as, e.g., CdTe or GaAs) by substituting a controlled fraction of nonmagnetic cations with magnetic ions (Mn, Fe, Eu . . .). One well-known DMS family, intensively studied for more than two decades, includes materials based on the II-VI compounds.² However, even though the II-VI-based DMS alloys exhibit a range of highly interesting properties, they are not good for spintronics applications because they are all antiferromagnetic. Yet, recent progress in the molecular-beam epitaxy growth of III-V-type DMS (such as GaMnAs, InMnAs, GaMnN),³ raises new hope, since they seem to possess all necessary features of a good spintronics material. In particular, the strongly *p*-type InMnAs and GaMnAs exhibit the desired FM behavior.⁴ The Curie points of these materials are still much below room temperature, which limits their practicality. Nevertheless, they may play an important role in developing prototypes of future spintronic devices.

The most desirable situation from the spintronics viewpoint is spontaneous formation of a single-domain FM state,

thus reducing the need for an external magnetic field. Our current insight into the domain structure of the new epitaxial ferromagnets is still insufficient. In general, the present knowledge of GaMnAs ferromagnetism is based on magnetization and transport measurements, which probe only the volume properties of the spin system.^{4,5} In principle, the FM behavior seen in those experiments may result from isolated FM aggregates/domains. In other words, such data do not provide conclusive information about the *range* of the FM ordering. Insight into this issue can be obtained only by methods capable of probing the magnetic correlations on a microscopic level. Neutron scattering which is known to be particularly well suited for that purpose is a much better way to study the magnetic order of DMS. In this paper we report neutron reflectometry data from GaMnAs/GaAs superlattices. By applying the technique of polarization analysis we were able to observe the magnetic scattering contributions from domain states. The results show that in most samples, cooling through the Curie temperature in zero external field leads to the formation of *single-domain* ferromagnetic order in the multilayered structure. Such behavior clearly indicates that the ferromagnetism occurring in individual GaMnAs layers is truly long range. Furthermore, the reflectometry data prove that there is significant exchange coupling between the GaMnAs layers across the intervening nonmagnetic GaAs spacers.

Another neutron scattering tool, known to be particularly well suited for probing microscopic spin-spin correlations in magnetic systems, is the conventional “wide-angle” diffraction. With the presently available GaMnAs samples, the application of this latter technique appears problematic. Since the volume of the material in these epitaxially grown specimens is extremely small, and the Mn atoms occupy only a small fraction of the lattice sites, the intensity of the magnetic diffraction signal is extremely weak. An additional complication is the fact that the films are deposited on pure GaAs which has almost the same lattice periodicity as GaMnAs. Therefore, the magnetic peaks occur at the same positions as the overwhelmingly stronger (10^3 – 10^4 times)

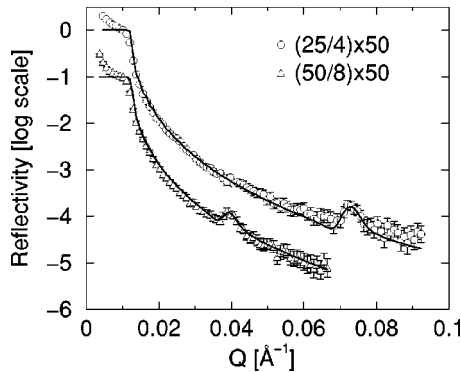


FIG. 1. Unpolarized neutron reflectivity profiles for $(25\text{ML}/4\text{ML}) \times 50$ and $(50\text{ML}/8\text{ML}) \times 50$ GaMnAs/GaAs superlattices. The solid lines represent theoretical reflectivity profiles calculated from the scattering length density contrast between GaMnAs and GaAs. Below the critical angle for total reflection the influence of the incident beam is seen due to the relaxed resolution of the instrument.

Bragg reflections from the substrate. Extracting the pure magnetic diffraction component from such data is extremely difficult. Rather, wide-angle diffraction studies of GaMnAs may become realistic only when semibulk self-supporting specimens become available. In reflectometry measurements, however, one uses samples in the form of GaMnAs/GaAs superlattices. Peaks in neutron reflectivity occur at positions corresponding to the superlattice periodicity, so that scattering from the substrate does not pose a problem. The magnetic and nuclear scattering components in the reflectivity maxima are of comparable intensity, and the latter component can be completely cut off using polarization analysis.

The SL samples for the present study were grown by molecular beam epitaxy on GaAs (001) substrates. The Mn concentration in the GaMnAs layers was 6%. In various samples investigated the GaMnAs layer thickness was 25 or 50 monolayers, and the GaAs spacer thickness was 4, 6 or 8 monolayers. The number of repeats in all samples was 50. The reflecting surface area of the samples was of the order of $1\text{--}1.5\text{ cm}^2$. As probed by magnetization measurements, the samples were ferromagnetic below $\sim 30\text{ K}$ (the details of the growth procedure and the magnetic characterization are presented elsewhere⁶).

Neutron reflectivity measurements were carried out at the NIST Center for Neutron Research using the NG-1 reflectometer in both polarized and unpolarized operation modes. The neutron wavelength was $\lambda = 4.75\text{ \AA}$. In the polarized mode all four types of the cross sections, corresponding to spin-flip (SF) and non-spin-flip (NSF) scattering processes were measured.

Typical reflectivity profiles from GaMnAs/GaAs superlattices taken with unpolarized neutron beam below T_C are shown in Fig. 1. Clearly visible are the first order superlattice Bragg peaks, their positions agreeing very well with the SL periodicity “targeted” in the growth process. The solid curves in the Fig. 1 represent the reflectivity profiles calculated from the scattering length density (SLD) contrast between GaMnAs and GaAs layers assuming Mn concentration $c_{\text{Mn}} = 0.06$.

TABLE I. Scattering length densities (SLD) for GaMnAs and GaAs for both neutron spin eigenstates in 10^{-6} \AA^{-2} units.

GaMnAs(++)	GaMnAs(--)	GaMnAs(+)	GaAs
$N(\bar{b}-\bar{p})$	$N(\bar{b}+\bar{p})$	$N\bar{p}$	$N\bar{b}$
2.713	3.067	0.177	3.070

Even though 0.06 is close to the maximum attainable Mn concentration, it is still a relatively small value, and the SLD contrast between the constituent layers is quite weak. Consequently, the Bragg peak intensity is rather low. The overall peak intensity consists of the nuclear part, which is the dominant component, and the magnetic part. This latter component can be extracted from the data by subtracting the spectrum measured above T_C . However, the signal obtained in such a manner is heavily affected by statistical error. Fortunately, polarized neutron techniques offer the possibility of detecting very small magnetic scattering effects superimposed on much higher nuclear ones by taking advantage of the interference between the magnetic and nuclear contributions to the scattering (e.g., Ref. 7). Another great advantage of a polarized neutron beam is its ability to sense the direction of the in-plane layer magnetization, and thus to probe separately different domain populations.

In the kinematic limit the four structure factors corresponding to NSF and SF scattering processes with the scattering vector \mathbf{Q} (normal to the specimen surface) can be described as follows:⁸

$$F^{\pm\pm} = \sum_j N_j (b_j \mp p_j \cos \phi_j) \exp(iQu_j), \quad (1)$$

$$F^{\pm\mp} = \sum_j N_j p_j \sin \phi_j \exp(iQu_j),$$

where the superscripts refer to the initial and final neutron spin eigenstates, b_j and p_j , respectively, are the average nuclear and magnetic scattering lengths for the j th atomic layer of the superlattice, N_j is its average atomic density, and u_j is the layer’s position along the axis parallel to \mathbf{Q} . ϕ_j denotes the angle between the polarization axis (parallel to the applied magnetic field) and the magnetic moment of the layer. This formulation is very useful for qualitative discussion of the experimental data. The magnetization component parallel to the applied field (vertical in our experiments) gives rise to NSF scattering [(++) or (--) in our notation] which interferes with the nuclear scattering [this is described by $b_j \mp p_j \cos \phi_j$ in the first of Eqs. (1)]. The perpendicular component (horizontal in our arrangement) is the source of purely magnetic, SF scattering. Table I shows the calculated scattering length densities for the superlattice constituents for the (++) and (--) NSF scattering cross sections and the (+) SF scattering cross section. Due to the negative value of $b_{\text{Mn}} = -3.73\text{ fm}$ and positive magnetic contribution from the $S = \frac{5}{2}$ Mn spin⁹ there is almost a perfect compensation of the SLD contrast between GaAs and magnetized GaMnAs for the (--) NSF cross section. Conse-

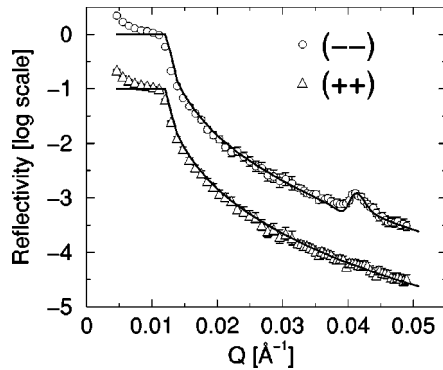


FIG. 2. Polarized NSF neutron reflectivity profiles for $(50\text{ML}/6\text{ML}) \times 50$ GaMnAs/GaAs superlattice taken at 2 G applied magnetic field. The data for $(++)$ scattering process is shifted an order of magnitude down for the figure clarity. The presence of the SL peak in $(--)$ and not in $(++)$ indicates that the layer magnetization is opposite to the applied magnetic field, i.e., the angles ϕ_j in Eq. (1) are equal to π .

quently for this neutron spin direction there should be no observable superlattice Bragg peak (see Fig. 2). For the other neutron polarization state the SL peak is enhanced as compared with the unpolarized neutron experiment.

Both the $(++)$ and $(--)$ NSF reflectivity profiles obtained for a GaMnAs/GaAs $(50\text{ML}/6\text{ML}) \times 50$ specimen are shown in Fig. 2. The absence of the SL Bragg peak in the $(++)$ data and its presence in the $(--)$ data indicate that the layer moments are aligned in the direction opposite to the applied magnetic field [i.e. all the ϕ_j angles in Eqs. (1) are equal to π].

The solid curves in Figs. 1 and 2 show theoretical reflectivities obtained by applying the optical treatment of the reflection process from a stratified homogeneous medium.¹⁰ In this approach the total reflectivity of the SL structure is calculated recursively from the reflection coefficients of each individual interface. Excellent agreement between calculated and experimental reflectivity profiles has been achieved using the SLD values listed in Table I.

In Fig. 3 we present a closer look at the first-order superlattice Bragg peak. The results for all four NSF and SF scattering processes are displayed for experiments performed below and above T_C and in applied external fields of 2 and 100 G. The panels (a), (b), (c) present the data in the same order the measurements were performed. However, for greater clarity, we discuss them in the reversed order. Above T_C [Fig. 3(c)] the sample is nonmagnetic (paramagnetic). As expected, both $(++)$ and $(--)$ cross section coincide since only nuclear scattering is present. There is also no spin-flip scattering. After cooling the sample down to 7.8 K and applying a 100 G external field [Fig. 3(b)] the sample is magnetically saturated [typical saturating field values for GaMnAs are several tens of G (Ref. 11)] and its magnetization is aligned parallel to the magnetic field. There is a SL Bragg peak in the $(++)$ cross section and no such peak in the $(--)$ data as one should expect considering Eq. (1) and the SLD values in Table I. For the saturated sample one should not expect any spin-flip scattering as there is no magnetization component perpendicular to the applied field. The

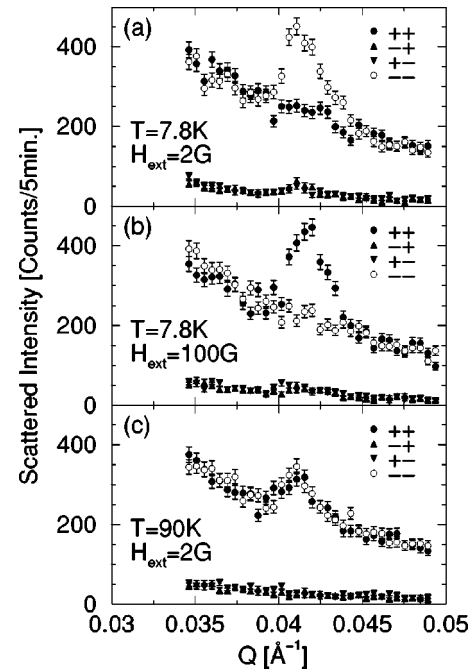


FIG. 3. Polarized neutron diffraction profiles about the first order SL Bragg peak for $(50\text{ML}/6\text{ML}) \times 50$ GaMnAs/GaAs superlattice. Non-spin-flip scattering processes $(++)$ and $(--)$ as well as spin-flip ones $(-+)$ and $(+-)$ are presented. No peak in spin-flip scattering indicates the absence of any horizontal component of the sample magnetization. Note the swap in the $(++)$ and $(--)$ scattering [see (a) and (b)] after applying an external magnetic field of 100 G.

most important result of this communication is presented in Fig. 3(a) which displays the reflectivity spectra measured after initially cooling the sample below T_C in zero external field. The peak of nearly identical profile as that seen in Fig. 3(b) clearly indicates that here also the sample is aligned with its full moment. It should be noted that during this measurement the field at the sample site was not exactly zero (as it was during the cooling process which took place before putting the sample cryostat on the reflectometer) but ~ 2 G, due to the reflectometer “guide fields.” However, this weak field has the same orientation as the external field used in our experiments, whereas the direction of the sample magnetization is reversed as compared to the situation depicted in Fig. 3(b) [the peak appears in the $(--)$ NSF scattering process]. Thus, the observed magnetization is certainly not a field-induced effect, but a spontaneous one, resulting only from cooling the sample below T_C . Moreover, the absence of $(++)$ NSF and SF scattering shows there are no domains with other magnetization orientation in the specimen, at least with dimensions of the order of or greater than the effective lateral coherence length of the neutron (in this case $\sim 100 \mu\text{m}$). A collection of randomly oriented domains of size less than the coherence length would result in an averaged magnetization of zero, for example.

All other samples investigated by us exhibited essentially the same behavior — namely, cooling through T_C in zero external field resulted in the formation of a single-domain

state — except for one specimen, in which all four possible domain states were populated.

The above observations lead to the following important conclusions: (i) in most cases, each GaMnAs layer spontaneously forms a single ferromagnetic domain and that the FM order in the GaMnAs is truly long range. (ii) the net magnetic moments in all constituent layers are parallel and ferromagnetically exchange coupled across the intervening spacers of nonmagnetic GaAs.

In summary, the presented polarized neutron reflectivity experiments prove that the ferromagnetic order within a single GaMnAs layer is of long range. The magnetization of each individual layer is spontaneously saturated (single domain). By comparing the intensities of the nuclear and magnetic contributions to the SL Bragg peak seen in the experiments with a nonpolarized beam, and taking into account the SLD contrast between GaMnAs and GaAs, we find that the

spin of the Mn ion is very close to $\frac{5}{2}$. It indicates that the range of the hole-mediated exchange interactions between the Mn ions is much larger than the average distance between these ions ($\sim 9 \text{ \AA}$). Also, our data provide clear evidence of ferromagnetic coupling between the GaMnAs layers, directly confirming the conclusions drawn from the analysis of magnetization hysteresis loops in earlier studies¹¹ of GaMnAs/GaAs/GaMnAs trilayers. The fact that the interlayer correlations occur in SL samples with GaAs spacers as thick as 8 monolayers is yet another evidence of the long range of the Mn-Mn exchange coupling forces.

This work was supported by the following projects: NATO PST.CLG 975228, NSF DMR-9510434, and KBN 2 P03B 154 18. We thank Dr. Julie Borchers for many enlightening discussions.

¹P. Ball, *Nature (London)* **404**, 918 (2000); J. De Boeck and G. Borghs, *Phys. World* **12**, 27 (1999).

²*Diluted Magnetic Semiconductors*, edited by J.K. Furdyna and J. Kossut (Academic, New York, 1988); *Diluted Magnetic Semiconductors*, edited by M. Balkanski and M. Averous (Plenum, New York, 1991).

³H. Ohno, *J. Magn. Magn. Mater.* **200**, 110 (1999), and references therein.

⁴H. Ohno, H. Munekata, T. Penney, S. von Molnar, and L.L. Chang, *Phys. Rev. Lett.* **68**, 2664 (1992); H. Ohno, *Science* **281**, 951 (1998), and references therein; T. Hayashi, M. Tanaka, T. Nishinaga, H. Shimada, H. Tsuchiya, and Y. Otsuka, *J. Cryst. Growth* **175/176**, 1063 (1997).

⁵F. Matsukura, H. Ohno, A. Shen, and Y. Sugawara, *Phys. Rev. B* **57**, R2037 (1998).

⁶J. Sadowski, J.Z. Domagala, J. Bąk-Misiuk, S. Kolesnik, K. Świątek, J. Kanski, and L. Ilver, *Thin Solid Films* **367**, 165 (2000).

⁷R.M. Moon, T. Riste, and W.C. Koehler, *Phys. Rev.* **181**, 920 (1969).

⁸C.F. Majkrzak, *Physica B* **173**, 75 (1991).

⁹J. Szczytko, A. Twardowski, K. Świątek, M. Palczewska, M. Tanaka, T. Hayashi, and K. Ando, *Phys. Rev. B* **60**, 8304 (1999).

¹⁰L.G. Parratt, *Phys. Rev.* **95**, 359 (1954).

¹¹N. Akiba, F. Matsukura, A. Shen, Y. Ohno, H. Ohno, A. Oiwa, S. Katsumoto, and Y. Iye, *Appl. Phys. Lett.* **73**, 2122 (1998).